https://doi.org/10.5194/egusphere-2024-414
Preprint. Discussion started: 6 September 2024

Investigating the celerity of propagation for small perturbations and dispersive sediment aggradation under a supercritical flow

Hasan Eslami[1], Erfan Poursoleymanzadeh[1], Mojtaba Hiteh[1,2], Keivan Tavakoli[1], Melika Yavari Nia[1,3], Ehsan Zadehali[1], Reihaneh Zarrabi[1,4], Alessio Radice[1]

[1]Dept. of Civil and Environmental Engineering, Politecnico di Milano, Milan, 20133, Italy
[2]Dept. Civil and Coastal Engineering, University of Florida, Gainesville, Florida 32611, US
[3]Dept. Soil, Water and Ecosystem Sciences, University of Florida, Gainesville, Florida 32611, US
[4]Dept. of Geography and Environment, University of Alabama, Tuscaloosa, Alabama 35487, US

Correspondence to: Alessio Radice (alessio.radice@polimi.it)

Abstract. The manuscript presents an investigation of the scales of propagation for sediment aggradation in an overloaded channel. The process has relevant implications for land protection, since bed aggradation reduces channel conveyance and thus increases inundation hazard; knowing the time needed for the aggradation to take place is important for undertaking suitable actions. Attention is here focused on supercritical flow, under which the process is dispersive and a depositional front cannot be clearly recognized; in these conditions, one needs to define propagation scales locally and instantaneously. Based on spatial and temporal rates of variation of the bed elevation we quantify a celerity of propagation for the sediment aggradation wave. Furthermore, considering that morphological processes are modeled by differential equations, the eigenvalues of the latter's system are the celerities of the so-called small perturbations. With reference to a laboratory experiment with temporally and spatially detailed measurements, and after a review of existing approaches to determine the celerity of small perturbations considering or discarding the concentration of transported sediment, the manuscript shows how the celerities of propagation correlate with one another, while their values differ by orders of magnitude. It is argued that accounting or not for the solid concentration in the governing equations does not significantly impact the correlation trends, even one of the eigenvalues changes significantly. Finally, a bulk value of a dimensionless aggradation celerity is provided, that can serve as a rule-of-thumb estimation, useful for engineering purposes.

1 Introduction

River sediment transport is one of the key processes shaping the Earth's surface and has a number of implications for human life (Dotterweich, 2008; Mazzorana et al., 2013; Haddadchi et al., 2014; Longoni et al., 2016; Pizarro et al., 2020). The morphologic evolution of rivers can be studied at a huge range of scales, the longest and shortest ones being related to geology/geomorphology and particle mechanics, respectively (e.g., Aksoy and Kavvas, 2005; Ancey, 2020, respectively). This paper is focused on the bed aggradation that results from an imbalance between an amount of supplied sediment and the transport capacity of the flow within a generic extreme event. The engineering relevance of this process has been demonstrated by a number of studies discussing how, during a calamitous event, sediment aggradation may increase hydraulic hazard (Sear et al., 1995; Stover and Montgomery, 2001; Lane et al., 2007; Radice et al., 2013). Sediment aggradation has been studied in the past for both the effects of pulsed sediment supply (e.g., Cui et al., 2003; Cui and Parker, 2005; Sklar et al., 2009) and the formation of depositional fronts (e.g., Soni, 1981; Yen et al., 1992; Alves and Cardoso, 1999; Zanchi and Radice, 2021). Besides the magnitude of morphologic changes, the scales of the progressive evolution of the process are also important. In fact, when a channel is overloaded with sediment, an aggradation wave propagates with a certain celerity along the reach. Knowing the celerity of propagation is crucial for estimating when an aggradation wave will reach any key spot along the stream.

Aggrading fronts induced by sediment overloading may be either translational or dispersive (Lisle et al., 2001). A translational front appears as a sharp discontinuity in the bed elevation. In a dispersive process, instead, a depositional wedge becomes

https://doi.org/10.5194/egusphere-2024-414
Preprint. Discussion started: 6 September 2024

progressively longer and thinner downstream. Zanchi and Radice (2021), based on laboratory experiments in subcritical conditions, could estimate the celerity of the aggradation wave by applying a tracing method since the sediment front was translational and therefore detectable in the performed experiments. They argued that translational features are favored by low Froude number and high overloading ratio (the ratio between the sediment inflow discharge and the initial sediment transport capacity of the flow), the opposite holding for dispersive features. In a supercritical flow, given a relatively high value of the Froude number, one expects a dispersive process to take place. In such a condition, due to the absence of a sharp sediment front, it is not possible to track the latter to estimate the celerity of propagation of the aggradation wave. Therefore, alternative methods are needed. The present manuscript indeed considers sediment aggradation in supercritical flow with the purpose of investigating its propagations scales, as most (if not all) prior investigations have been conducted for subcritical conditions.

From a mathematical point of view, several studies have been performed to simulate the sediment transport process in rivers by using a quasi-two-phase approach in a one-dimensional framework (for example, De Vries, 1965, 1971, 1973, 1993; Armanini and Di Silvio, 1988; Sieben, 1997, 1999; Kassem and Chaudry, 1998; Lyn and Altinakar, 2002; Lee and Hsieh, 2003; Rosatti et al., 2005; Rosatti and Fraccarollo, 2006; Goutière et al., 2008; Armanini et al., 2009; Garegnani et al., 2011; Armanini, 2018). In a quasi-two-phase approach, the hydro-morphologic evolution of the bed and water surfaces is depicted by a hyperbolic system of partial differential equations, including mass and momentum conservation equations for the mixture phase and one continuity equation (the Exner equation) for the sediment phase. When the volumetric concentration of the transported sediment (that is the ratio of sediment discharge to the water-sediment mixture discharge) is negligible, this system may be transformed into another one containing mass and momentum conservation equations for the clear water (i.e., the Saint-Venant equations) and the Exner equation. De Vries (1965) proposed to consider the sediment concentration negligible below a threshold value of around 0.002, while Garegnani et al. (2011, 2013) introduced a higher threshold of 0.01. However, several authors have argued that the eigenvalues of the hyperbolic system represent the celerity of propagation of small perturbations in bed and water. Furthermore, some studies have proposed approximate determinations of the eigenvalues of a simplified system of equations for negligible sediment concentration (De Vries, 1965, 1971, 1973; Lyn, 1987; Lyn and Altinakar, 2002; Goutière et al., 2008; Armanini, 2018); by contrast, Morris and Williams (1996) argued that the assumption of a negligible concentration is not appropriate for many natural streams and, based on that, provided an equation to estimate the eigenvalues of the full system of equations.

The celerity of propagation of small perturbations is not the celerity of propagation of the aggradation wave, as also happens considering water in a fixed-bed flood wave model. Therefore, if one needs to provide a celerity for the sediment involved in the aggradation process, something different is needed and may be quantified considering the spatial and temporal rate of variation of the bed elevation. A key objective of the present study is investigating the correlation between the celerity of propagation of the aggradation wave (determined as just mentioned) and the celerity of small perturbations (determined as the eigenvalues of the system.

Based on the arguments above, the present manuscript is articulated around the following questions: (1) How can one quantify the scales of propagation in an aggradation process? (2) What is the relationship between the aggradation celerity and the celerity of small perturbations? and finally (3) Which is the impact of considering or not the sediment concentration on the previous point? These issues are investigated with reference to an aggradation experiment performed in a laboratory flume. The manuscript is structured as follows: Section 2 provides a review of how the eigenvalues of the hyperbolic equations have been treated by several studies with or without an assumption of negligible sediment concentration. Section 3 shows how one may estimate the local and instantaneous celerity of propagation. In section 4, the experimental setup and the measurement techniques are presented; furthermore, the methods for the quantitative determination, based on the measurement of the bed elevation, of the scales of propagation are described. Sections 5 and 6 contain the experimental results and a discussion, respectively. Finally, the key conclusions of the study are provided.

https://doi.org/10.5194/egusphere-2024-414
Preprint. Discussion started: 6 September 2024

2 Mathematical modeling of channel morphologic evolution: a review of quasi-two-phase approaches and the celerity of small perturbations

In a fully-two-phase approach, the governing equations for one-dimensional modeling of channel morphologic evolution comprehend four partial differential equations (e.g., Greco et al., 2012), including two mass and momentum equations for the mixture phase and the same equations for the solid phase. However, since in the literature a quasi-two-phase approach has been widely taken to simulate mobile-bed flows, we follow this approach also in this study. A quasi-two-phase model for river morphology is based on two main hypotheses (e.g., Garegnani et al., 2013). First, if the volumetric concentration of the transported sediment, c_s, does not exceed a certain value (for example, Armanini et al., 2009 proposed a threshold at 0.05), then the bed shear stress may be computed using the same equations one uses for clear-water conditions. Second, water and sediment move at almost the same velocity. As mentioned above, in a quasi-two-phase approach, due to the second assumption, a hyperbolic system of partial differential equations includes one continuity equation for the mixture, one momentum equation for the mixture, and one continuity equation for the bed sediment (Exner equation). The two equations for the mixture can be simplified to the well-known Saint-Venant equations for clear water if the solid concentration is negligible.

2.1 Governing equations and eigenvalue analysis for negligible c_s

Several authors (e.g., De Vries, 1965, 1971, 1973, 1993; Sieben, 1997, 1999; Armanini, 2018; Goutière et al., 2008; Garegnani et al., 2011, 2013) have argued that in fluvial environments the volumetric solid concentration may be assumed to be very small. With this assumption, the Saint-Venant and Exner equations are obtained for a unit-width rectangular channel as follows:

$$\begin{cases} \dfrac{\partial h}{\partial t} + \dfrac{\partial (uh)}{\partial x} = 0 \\ \dfrac{\partial (uh)}{\partial t} + \dfrac{\partial (u^2 h)}{\partial x} + gh\left(\dfrac{\partial h}{\partial x} + \dfrac{\partial z_b}{\partial x}\right) = -ghS_f \\ (1-p_0)\dfrac{\partial z_b}{\partial t} + \dfrac{\partial q_s}{\partial x} = 0 \end{cases} \tag{1}$$

where h = water depth; u = depth-averaged water velocity; g = gravity acceleration; z_b = bed elevation; S_f = friction slope; p_0 = bed porosity; and q_s = sediment discharge per unit width. This system contains five unknowns, namely h, u, z_b, S_f, q_s, and only three equations; therefore, in order to ensure the existence of a solution two other equations, working as closure relationships, are needed. The latter express S_f and q_s. For the friction slope, the Manning formula is frequently used:

$$S_f = \frac{n^2 \times u^2}{R_H^{4/3}} \tag{2}$$

where n = Manning's coefficient; and R_H = hydraulic radius. To evaluate the sediment discharge, q_s, many formulae are available. For example, Goutiére et al. (2008) expanded the formula of Meyer-Peter and Müller (1948) as follows:

$$q_s(q,h) = 8\sqrt{g(s-1)d_{50}^3}\left(\frac{n^2 q^2}{(s-1)d_{50}h^{7/3}} - 0.047\right)^{3/2} \tag{3}$$

where $q = uh$ = water discharge per unit width; $s = \rho_s/\rho$ = relative sediment density (ρ_s and ρ represent the sediment and water densities, respectively); and d_{50} = median grain diameter.

Exploiting a compound derivative for $\partial q_s/\partial x$ and the derivation of the product for $\partial(uh)/\partial x$, system (1) becomes:

https://doi.org/10.5194/egusphere-2024-414
Preprint. Discussion started: 6 September 2024

$$\begin{cases} \dfrac{\partial h}{\partial t} + u\,\dfrac{\partial h}{\partial x} + h\,\dfrac{\partial u}{\partial x} = 0 \\ \dfrac{\partial u}{\partial t} + g\dfrac{\partial h}{\partial x} + u\dfrac{\partial u}{\partial x} + g\dfrac{\partial z_b}{\partial x} = -gS_f \\ \dfrac{\partial z_b}{\partial t} + \dfrac{1}{(1-p_0)}\dfrac{\partial q_s}{\partial h}\dfrac{\partial h}{\partial x} + \dfrac{1}{(1-p_0)}\dfrac{\partial q_s}{\partial u}\dfrac{\partial u}{\partial x} = 0 \end{cases} \tag{4}$$

System (4) can be written in the vector form as (Armanini, 2018):

$$\frac{\partial \boldsymbol{U}}{\partial \boldsymbol{t}} + \boldsymbol{A_U}\frac{\partial \boldsymbol{U}}{\partial \boldsymbol{x}} + \boldsymbol{S_U} = 0 \tag{5}$$

where:

$$\boldsymbol{U} = \begin{bmatrix} h \\ u \\ z_b \end{bmatrix} \qquad \boldsymbol{A_U} = \begin{bmatrix} u & h & 0 \\ g & u & g \\ \frac{1}{(1-p_0)}\frac{\partial q_s}{\partial h} & \frac{1}{(1-p_0)}\frac{\partial q_s}{\partial u} & 0 \end{bmatrix} \qquad \boldsymbol{S_U} = \begin{bmatrix} 0 \\ gS_f \\ 0 \end{bmatrix} \tag{6}$$

are the vector of unknowns, the matrix of coefficients, and the vector of known terms, respectively.

One can then determine the eigenvalues (λ_1, λ_2, and λ_3) of the coefficient matrix, $\boldsymbol{A_U}$, that represent the slope of the so-called characteristic curves and, according to the literature (De Vries, 1965, 1971, 1973; Lyn, 1987; Lyn and Altinakar, 2002; Goutière et al., 2008; Armanini, 2018), the celerity of propagation of small perturbations in the bed and water surfaces. The three eigenvalues of the system can be obtained by solving the following equation:

$$det(\boldsymbol{A_U} - \lambda \boldsymbol{I}) = \boldsymbol{0} \tag{7}$$

where $\boldsymbol{I}$ is the identity matrix. By developing (7) one obtains a cubic equation which is known as the characteristic polynomial equation (Armanini, 2018):

$$p(\lambda) = -\lambda^3 + 2u\lambda^2 + (gh - u^2 + ghA_\lambda)\lambda - ghu(A_\lambda - B_\lambda) = 0 \tag{8}$$

where:

$$A_\lambda = \frac{1}{(1-p_0)h}\frac{\partial q_s}{\partial u} \quad , \quad B_\lambda = \frac{1}{(1-p_0)u}\frac{\partial q_s}{\partial h} \tag{9}$$

are dimensionless parameters. Though the three real and distinct eigenvalues (Rosatti and Fraccarollo, 2006) of the system can be computed exactly by solving this cubic equation, approximated solutions may be useful for interpretation purposes (Lyn, 1987). Numerous studies have thus been performed to investigate the characteristic curves (Lyn and Altinakar, 2002) and to present approximated formulations for λ_1, λ_2, and λ_3. In the following, some of them are reviewed.

2.1.1 De Vries' approach

De Vries (1965, 1971, 1973, 1993) referred to the eigenvalues of the system as the "celerities of the surface and bed waves in mobile-bed flows". To estimate them, he proposed an approximated solution valid for Froude numbers (Fr) lower than 0.8 or higher than 1.2:

$$\begin{cases} \lambda_1 \cong \left[1 + \dfrac{1}{Fr}\right]u \\ \lambda_2 \cong \left[1 - \dfrac{1}{Fr}\right]u \\ \lambda_3 \cong \dfrac{u}{1 - Fr^2}(A_\lambda - B_\lambda) \end{cases} \tag{10}$$

In Eq. (10), one recognizes that λ_1 and λ_2 are the well-known surface wave celerities for the Saint-Venant equations representing water flow. In this approach, therefore, for a flow sufficiently distant from the critical conditions and negligible

https://doi.org/10.5194/egusphere-2024-414
Preprint. Discussion started: 6 September 2024

solid concentration, the first two eigenvalues are not affected by the presence of sediment transport. Instead, λ_3 was considered as the celerity of the bed surface perturbations.

The eigenvalues λ_2 and λ_3 have a different sign in subcritical and supercritical flow. Therefore, an alternative version of Eq. (10) has been proposed to obtain eigenvalues with the same sign ($\lambda_1 > 0$, $\lambda_2 < 0$, $\lambda_3 > 0$) for both the flow conditions:

$$Fr < 0.8 \begin{cases} \lambda_1 \cong \left[1 + \frac{1}{Fr}\right] u \\ \lambda_2 \cong \left[1 - \frac{1}{Fr}\right] u \\ \lambda_3 \cong \frac{u}{1 - Fr^2}(A_\lambda - B_\lambda) \end{cases} \qquad Fr > 1.2 \begin{cases} \lambda_1 \cong \left[1 + \frac{1}{Fr}\right] u \\ \lambda_2 \cong \frac{u}{1 - Fr^2}(A_\lambda - B_\lambda) \\ \lambda_3 \cong \left[1 - \frac{1}{Fr}\right] u \end{cases} \tag{11}$$

2.1.2 Lyn and Altinakar's approach

Lyn (1987), then followed by Lyn and Altinakar (2002), presented different approximations to estimate the three eigenvalues for near-critical flows ($0.8 \leq Fr^2 \leq 1.2$):

$$\begin{cases} \lambda_1 \cong \left[\frac{3}{2} + \frac{1}{2Fr}\right] u \\ \lambda_2 \cong \left[\frac{1}{4}\left(1 - \frac{1}{Fr^2}\right) - \frac{1}{4}\sqrt{\left(1 - \frac{1}{Fr^2}\right)^2 + \frac{8A_\lambda}{Fr^2}}\right] u \\ \lambda_3 \cong \left[\frac{1}{4}\left(1 - \frac{1}{Fr^2}\right) + \frac{1}{4}\sqrt{\left(1 - \frac{1}{Fr^2}\right)^2 + \frac{8A_\lambda}{Fr^2}}\right] u \end{cases} \tag{12}$$

Lyn and Altinakar (2002) argued that λ_2 and λ_3 are not devoted merely to a surface wave or a bed wave but, rather, they represent the celerity of propagation of both surface and bed waves. This finding is somehow consistent with Sieben's (1997, 1999) statement that in near-critical regimes the bed waves interact strongly with the surface waves.

2.1.3 Goutière et al.'s approach

Goutière et al. (2008) developed approximated formulations for the eigenvalues of a system of partial differential equations slightly different from (1), where h, q and z_b were the main dependent variables:

$$\begin{cases} \frac{\partial h}{\partial t} + \frac{\partial q}{\partial x} = 0 \\ \frac{\partial q}{\partial t} + \frac{\partial}{\partial x}\left(\frac{q^2}{h}\right) + gh\left(\frac{\partial h}{\partial x} + \frac{\partial z_b}{\partial x}\right) = -ghS_f \\ (1 - p_0)\frac{\partial z_b}{\partial t} + \frac{\partial q_s}{\partial x} = 0 \end{cases} \tag{13}$$

To estimate the three eigenvalues of the system they proposed the following equations:

$$\begin{cases} \lambda_1 \cong \left[1 + \frac{1}{Fr}\right] u \\ \lambda_2 \cong \frac{1}{2}\left[\left(1 - \frac{1}{Fr}\right) - \sqrt{\left(1 - \frac{1}{Fr}\right)^2 - \frac{4(A_\lambda - B_\lambda)}{(Fr^2 + Fr)}}\right] u \\ \lambda_3 \cong \frac{1}{2}\left[\left(1 - \frac{1}{Fr}\right) + \sqrt{\left(1 - \frac{1}{Fr}\right)^2 - \frac{4(A_\lambda - B_\lambda)}{(Fr^2 + F_r)}}\right] u \end{cases} \tag{14}$$

Differently from the approaches of De Vries and Lyn and Altinakar, Eq. (14) are to be intended as valid for the whole range of Froude numbers.

https://doi.org/10.5194/egusphere-2024-414
Preprint. Discussion started: 6 September 2024

2.2 Governing equations and eigenvalue analysis for non-negligible c_s

Morris and Williams (1996) argued that an assumption of negligible solid concentration is not appropriate for many natural streams and, therefore, determined the eigenvalues of a system of equations considering a finite c_s. The continuity and momentum equations of the mixture and the continuity equation for the sediment in Morris and Williams' approach are as follows:

$$\begin{cases} \dfrac{\partial(uh)}{\partial x}+\dfrac{\partial h}{\partial t}+\dfrac{\partial z_b}{\partial t}=0 \\ \dfrac{\partial u}{\partial t}+u\dfrac{\partial u}{\partial x}+g\dfrac{\partial h}{\partial x}+\dfrac{(\rho_s-\rho)gh}{2\rho_m}\dfrac{\partial c_s}{\partial x}-\dfrac{[(1-p_0)\rho_s+p_0\rho]u}{\rho_m h}\dfrac{\partial z_b}{\partial t}+g\dfrac{\partial z_b}{\partial x}=-gS_f \\ \dfrac{\partial(uhc_s)}{\partial x}+\dfrac{\partial(hc_s)}{\partial t}+(1-p_0)\dfrac{\partial z_b}{\partial t}=0 \end{cases} \tag{15}$$

where, $c_s=q_s/(q_s+q)$, and $\rho_m=c_s\rho_s+(1-c_s)\rho$ is the density of the mixture. Since the solid concentration is not negligible, the water and sediment discharge per unit width are obtained from the following equations (always assuming that the solid particles move with the same velocity of water):

$$q=uh(1-c_s) \tag{16}$$

$$q_s=uhc_s \tag{17}$$

The system can be again closed using Eq. (2) and Eq. (3), as the latter furnishes a mean to compute c_s from Eq. (17).
The eigenvalues of the system (15) are determined by solving the following cubic equation (for the sake of completeness, an extended report of Morris and Williams' derivations is included in Supplemental 1):

$$\begin{aligned} &\lambda^3\left\{Bu\tfrac{\partial c_s}{\partial u}-h\tfrac{\partial c_s}{\partial h}-[c_s-(1-p_0)]\right\}+\lambda^2\left(\{Agh[c_s-(1-p_0)]-2Bu^2\}\tfrac{\partial c_s}{\partial u}+(2+B)uh\tfrac{\partial c_s}{\partial h}+\right.\\ &\left.2u[c_s-(1-p_0)]\right)+\lambda\left[(Bu^3-ugh\{1+A[c_s-(1-p_0)]\})\tfrac{\partial c_s}{\partial u}-\left((1+B)u^2h-gh^2\{1+\right.\right.\\ &\left.\left.A[c_s-(1-p_0)]\}\right)\tfrac{\partial c_s}{\partial h}-(u^2-gh)[c_s-(1-p_0)]\right]+ugh\left(u\tfrac{\partial c_s}{\partial u}-h\tfrac{\partial c_s}{\partial h}\right)=0 \end{aligned} \tag{18}$$

where $A=(\rho_s-\rho)/(2\rho_m)$ and $B=\left((1-p_0)\rho_s+p_0\rho\right)/\rho_m$ are dimensionless parameters. Differently from the previous approaches for negligible c_s, this last one does not carry explicit approximated equations for the λ values.

3 Estimation of the local and instantaneous celerity of propagation of sediment aggradation

To determine the celerity of propagation of a certain quantity X, that varies in space and time, one can borrow the developments provided for unsteady flow by, for example, Chow et al. (1988) or Jain (2001). The celerity of propagation is defined as the velocity at which a given value of that quantity migrates along the system with respect to a still observer or, conversely, the velocity that an observer needs to move at to see a constant value for the quantity. One can thus obtain the celerity of propagation of X as follows:

$$\frac{\mathrm{d}X}{\mathrm{d}t}=\frac{\partial X}{\partial t}+\frac{\partial X}{\partial x}\frac{\mathrm{d}x}{\mathrm{d}t}=0\ \rightarrow C_X=\frac{dx}{dt}=-\frac{\partial X/\partial t}{\partial X/\partial x} \tag{19}$$

In a clear-water wave model, suitable quantities to be used as X are, for example, water depth or discharge. In the present case, any quantity related to the morphologic process may be used; in the next section we will motivate a choice of using the bed elevation, after a presentation of the experimental methods.

https://doi.org/10.5194/egusphere-2024-414
Preprint. Discussion started: 6 September 2024

4 Materials and methods

The aggradation experiment presented in this paper has been run at the Mountain Hydraulics Laboratory of the Politecnico di Milano, Lecco campus (Italy). The experimental setup and procedures are briefly reported below, referring to prior work for details.

4.1 Experimental setup, procedures, and measuring methods

The configuration of the used flume is shown in Fig. 1. The flume has a length of 5.2 m, a width of 0.3 m, a bank height of 0.45 m, and is entirely made of Plexiglas. The water discharge, Q, pumped from an underground container into an upstream tank, is adjusted using a guillotine valve and measured by an electromagnetic flowmeter. The erodible channel bed has a thickness of 0.15 m and is made of Polyvinyl Chloride (PVC), uniform sediment cylinders with a density ρ_s of 1443 kg/m^3, an equivalent diameter (computed for a sphere with the same volume of a cylinder) d of 3.8 mm, porosity p_0 of 0.45 (Unigarro Villota, 2017), and a Manning roughness coefficient n of 0.015 s/m$^{1/3}$ (as determined during preliminary tests by Zanchi and Radice, 2021). A sediment feeding system with a vibrating channel and a hopper is employed upstream. At the downstream end, the channel is equipped with sediment collectors. The bed is fixed in an upstream and a downstream portion to avoid undesired scour. A laser distance sensor is installed to continuously measure the water elevation in the inlet tank.

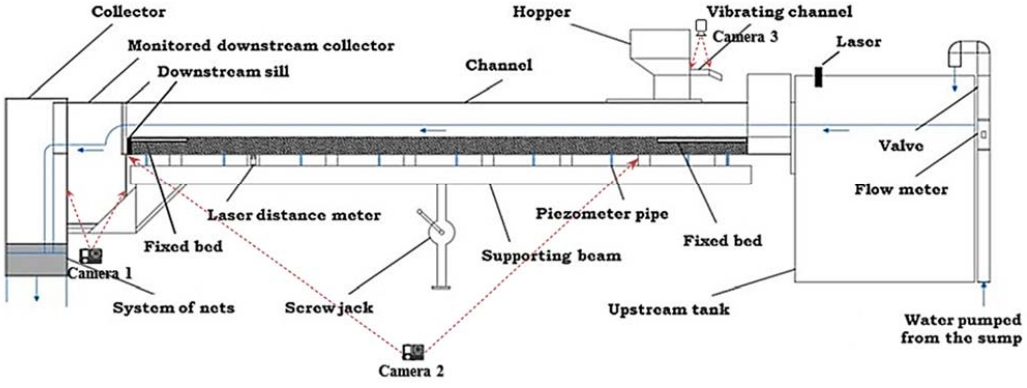

Figure 1. Flume used for the aggradation experiment. Camera 1 shoots the collector; camera 2 shoots the channel from the side; camera 3 shoots the vibrating channel of the sediment feeding system.

Prior to executing an experiment, the sediment bed is leveled and sprayed with water to avoid surface tension effects at water arrival. Then, the water pumping system is switched on and the flume is filled at negligible discharge to avoid any significant disturbance to the sediment. In this term, several cameras placed around the flume (see again Fig. 1) are turned on. After saturation of the bed, which typically takes some minutes, the water discharge is increased to the test value in roughly one minute; in this phase, the continuous reading of the discharge measured by the flowmeter and the laser measurement of the water elevation in the inlet tank furnish the necessary data to compute the temporal evolution of the flow rate entering the flume. When the sediment in the flume starts being transported, the sediment feeding is activated (the time at which the feeder is turned on is considered the initial time of the experiment). During the experiment, the hopper is refilled manually, and the experiment ends when no more sediment material is available (the duration of the aggradation phase is generally less than 10 minutes).

All the measurements are taken by image analysis, using the videos acquired by the various cameras. First, the sediment feeding rate, Q_{s-in}, is obtained from the videos recorded by camera 3 placed above the vibrating channel. Particle image velocimetry is used to measure the velocity of the particles moving along the vibrating channel; then, this velocity is converted into a sediment feeding rate using a predetermined transfer function (for details on the calibration of the method the reader can refer to Radice and Zanchi, 2018).

https://doi.org/10.5194/egusphere-2024-414
Preprint. Discussion started: 6 September 2024

Second, in order to measure the bed and water elevation during the experiment, a motion-detection method is applied to the videos captured by camera 2 placed beside the channel. For the measurement of the bed elevation, this method is based on the concept that the bed-load layer is part of the mixture flow while the bed is atop the still sediment in the bottom layer; according to that, the bed is located at the maximum elevation where no sediment motion occurs (see Eslami et al., 2022). For the measurement of the water surface elevation, instead, the method relies on detecting the motion of sediment particles sparsely transported within the flow. Two subsequent frames of the movie are subtracted from each other and imposing a threshold value to the resulting difference determines the border between motion and stillness; the upper and lower edges of the detected motion layer are considered as the water and bed surface elevations, respectively. The method has been validated against manual measurements taken during the experimental campaign that includes the run presented in this manuscript.

Third, the sediment transport capacity of the initial flow, Q_{s0}, is measured by two methods, one relying on the sediment volume progressively accumulated into the downstream collector and one obtaining the sediment volume leaving the flume from those fed and accumulated in the channel (thus applying the mass conservation principle). Full details are also provided in Eslami et al. (2022). The measurement of Q_{s0} is necessary to obtain the sediment overloading ratio $Lr = Q_{s-in}/Q_{s0}$.

4.2 Aggradation experiment and raw results

Table 1 lists the control parameters of the aggradation experiment performed in the current work (symbols not already defined in the text include T as the experiment duration, S_0 as the initial channel slope, and Q as the flow rate).

Table 1. Parameters of the aggradation experiment performed in the present study.

$T\ (s)$	$S_0\ (\%)$	$Q\ (l/s)$	$Q_{s-in}\ (m^3/s)$	$Q_{s0}\ (m^3/s)$	Lr
316	1.37	7.0	4.28×10^{-4}	1.33×10^{-4}	3.2

Figures 2(a) and 2(b) present the spatial evolution profiles of the bed and water surface at some specific time instants for the performed experiment. The profiles are provided from the x-coordinate (increasing from upstream to downstream) equal to 140 cm (distance from the upstream) because the channel is monitored by the camera from this coordinate (it should be mentioned that the x-coordinate of the channel feeding point is equal to 30 cm). As it is evident from the bed surface profiles, a sediment front is not clearly detectable during the experiment, i.e., it is of a dispersive type, since the experiment was performed with a relatively high flow velocity. Furthermore, after a time of around 190 s, the profiles do not further evolve, indicating the achievement of an equilibrium condition.

https://doi.org/10.5194/egusphere-2024-414
Preprint. Discussion started: 6 September 2024

(a)

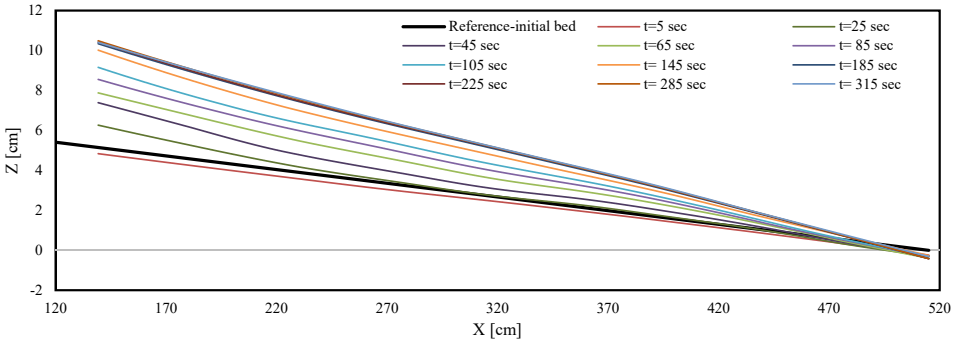

(b)

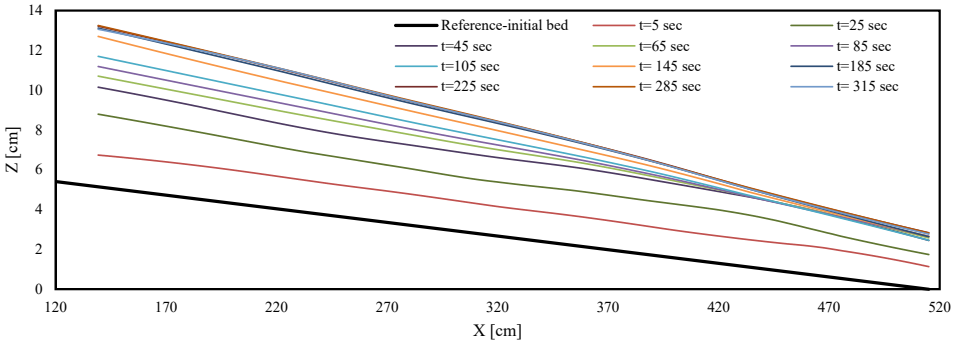

Figure 2. Spatial profiles of (a) bed elevation (b) water elevation, during the experiment.

Figure 3 depicts color gradient maps for the elevations of the bed and water surface, to appreciate spatial and temporal evolutions simultaneously. The contour lines become vertical for times larger than 190 s, again demonstrating the achievement of morphological equilibrium in the performed experiment.

Finally, Fig. 4 depicts the color gradient map of the Froude number, obtained from local and instantaneous velocity and depth. The Froude number was larger than 1 for most of the experiment (with a mean value of 1.3 for the entire map), corresponding to a supercritical flow condition.

https://doi.org/10.5194/egusphere-2024-414
Preprint. Discussion started: 6 September 2024

(a) (b)

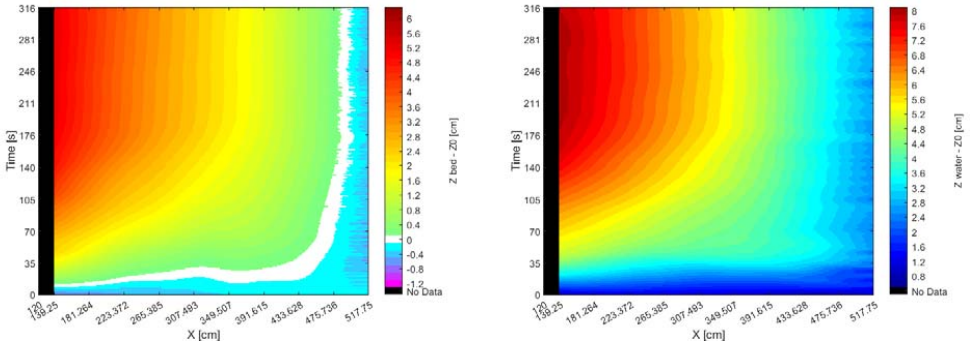

Figure 3. Color gradient maps of (a) bed elevation (b) water elevation, for the performed experiment.

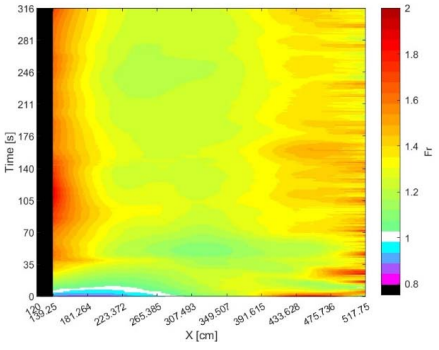

Figure 4. Color gradient map of Froude number for the performed experiment.

4.3 Estimation of the local and instantaneous celerity of propagation of sediment aggradation

Eq. (19) is applied to the bed elevation z_b that is the most suitable quantity to determine the celerity of the sediment wave. The bed elevation was preferred to, for example, the sediment transport rate because it was directly measured during the experiments with high spatial and temporal resolution. To exploit the equation for the present purposes, it was converted into a discrete form:

$$C = -\frac{\Delta z_b/\Delta t}{\Delta z_b/\Delta x} \tag{20}$$

where Δt and Δx are suitable time and space steps. In this work, Δt and Δx are chosen as equal to 1 s and 1.8 cm, respectively.

4.4 Eigenvalue determination using approaches for negligible and non-negligible sediment concentration

Within the approaches for negligible solid concentration, the equations proposed by Goutière et al. (2008) are used in this study, since these equations are valid for the entire range of the Froude number providing determinations very similar to those from the exact solution of Eq. (8). Since all the quantities involved in the eigenvalue determination vary in space and time, one obtains a corresponding space-time variation of the λ values. In order to make the eigenvalue determination fully consistent with the performed experiment, Eq. (3) was preliminarily calibrated introducing a bed-load factor α and an equivalent Manning coefficient accounting for sediment transport (excluding for simplicity the threshold Shields number from the calibration parameters):

https://doi.org/10.5194/egusphere-2024-414
Preprint. Discussion started: 6 September 2024

$$q_s(q,h) = \alpha 8\sqrt{g(s-1)d_{50}^3}\left(\frac{n_{calibrated}^2 q^2}{(s-1)d_{50}h^{7/3}} - 0.047\right)^{3/2} \quad (21)$$

Following Eslami et al. (2022), the calibration was performed by using Eq. (21) in a numerical simulation of the experiment and achieving a good consistency between experimental and numerical profiles of the bed and water surface. The values obtained for α and $n_{calibrated}$ are equal to 1.73 and 0.017 s/m$^{1/3}$, respectively. Furthermore, by substituting $q = uh$ in Eq. (21), explicit equations for $\partial q_s/\partial u$ and $\partial q_s/\partial h$ were obtained to determine A_λ and B_λ from Eq. (10). Finally, λ_1, λ_2, and λ_3 could be computed by Eq. (14).

There is no explicit equation in the literature to estimate λ_1, λ_2, and λ_3 for non-negligible solid concentration; therefore, in the current study, the eigenvalues were determined by finding the roots of Eq. (18). Since the sediment transport rate was expressed by Eq. (21), an equation for sediment concentration was obtained from that one as:

$$c_s(u,h) = \frac{8\alpha\sqrt{g(s-1)d_{50}^3}\left(\frac{n_{calibrated}^2 (uh(1-c_s))^2}{(s-1)d_{50}h^{7/3}} - 0.047\right)^{3/2}}{uh} \quad (22)$$

to be solved iteratively to determine c_s. Furthermore, Eq. (18) requires the derivatives $\partial c_s/\partial u$ and $\partial c_s/\partial h$, that were obtained introducing a function $F(u,h,c_s)$ as follows:

$$F(u,h,c_s) = \frac{8\alpha\sqrt{g(s-1)d_{50}^3}\left(\frac{n_{calibrated}^2 (uh(1-c_s))^2}{(s-1)d_{50}h^{7/3}} - 0.047\right)^{3/2}}{uh} - c_s \quad (23)$$

and, finally, determining the needed derivatives

$$\frac{\partial c_s}{\partial u} = -\frac{\partial F(u,h,c_s)/\partial u}{\partial F(u,h,c_s)/\partial c_s} \quad (24)$$

$$\frac{\partial c_s}{\partial h} = -\frac{\partial F(u,h,c_s)/\partial h}{\partial F(u,h,c_s)/\partial c_s} \quad (25)$$

5 Results

5.1 Local and instantaneous celerity of propagation of sediment aggradation

The color gradient map of C as obtained by Eq. (20) is depicted in Fig. 5(a) with a dimensionless counterpart (using the local and instantaneous flow velocity as a normalization parameter) in Fig. 5(b). The space-time distribution of the celerity values was smoothed by replacing any 64 values (8×8 values in space and time) with their average. This smoothing operation does not alter the key result but obviously provides a nicer plot for the following interpretation.

The local and instantaneous celerity evidently tends to reach a zero value at the time around 190 s, coinciding with the previously mentioned achievement of a morphologic equilibrium. While the average values of the celerity and dimensionless celerity by considering the whole duration of the experiment are equal to 0.393 cm/s and around 0.006, respectively, they are equal to 0.642 cm/s and 0.010 considering only times lower than 190 s (in both cases, all the locations along the channel are considered).

https://doi.org/10.5194/egusphere-2024-414
Preprint. Discussion started: 6 September 2024

(a) (b)

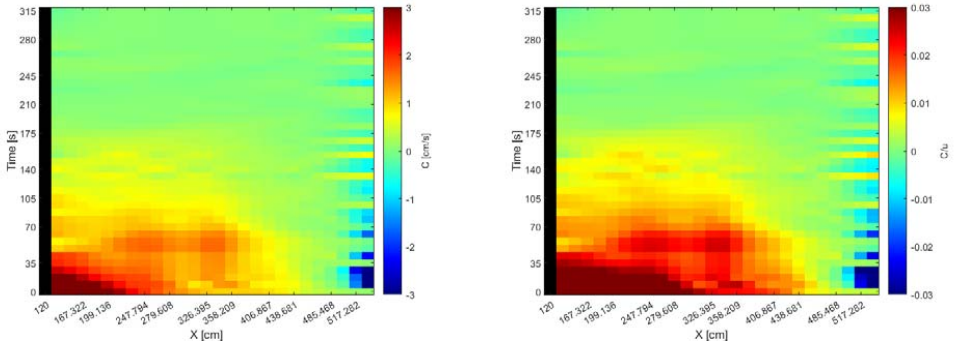

Figure 5. Smoothened color gradient maps of (a) dimensional and (b) dimensionless local and instantaneous celerity of propagation of sediment aggradation.

5.2 Eigenvalues of the system of PDEs

Figure 6(a, b, c) shows the color gradient maps of the dimensionless eigenvalues, $\lambda_1/u, \lambda_2/u,$ and λ_3/u, obtained from the approximated solutions proposed by Goutière et al. (2008) and from the exact solutions of the equation obtained by Morris and Williams (1996) (left and right panels, respectively). The smoothing, described above for the mass celerity, was also applied to these celerities of small perturbations. The average values of $\lambda_1/u, \lambda_2/u,$ and λ_3/u for the entire duration of the experiment and until the equilibrium time are equal to 1.77, -0.21 and 0.43 and to 1.77, -0.13 and 0.46, respectively, for the approaches of Goutière et al. (2008) and Morris and Williams (1996). Therefore, the values are quite similar for λ_1 and λ_3 while a significant difference is obtained for λ_2.

https://doi.org/10.5194/egusphere-2024-414
Preprint. Discussion started: 6 September 2024

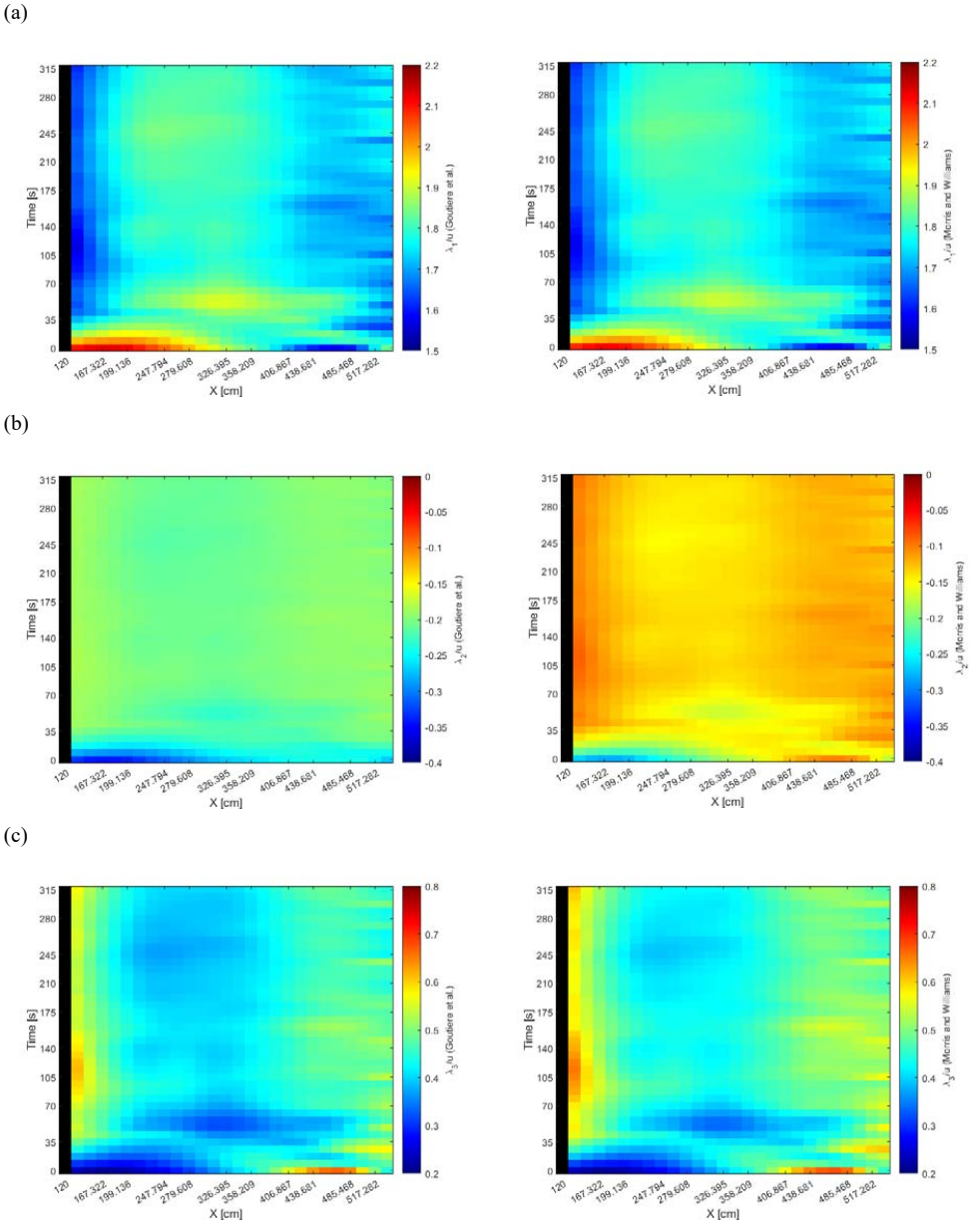

300 **Figure 6. Comparison between the smoothened color gradient maps of (a) λ_1/u, (b) λ_2/u and (c) λ_3/u. The left graphs are obtained from the approximated solutions proposed by Goutière et al. (2008) and the right graphs are derived from the exact solution of Morris and Williams' (1996) approach.**

5.3 Quantification of sediment concentration

The smoothed color gradient map of the volumetric sediment concentration as obtained using Eq. (22) is depicted in Fig. 7.
305 The average value of c_s for the whole duration of the experiment and also until the equilibrium time is around 0.032, indicating that, according to the criteria proposed by De Vries (1965) with maximum c_s=0.002 and by Garegnani et al. (2011, 2013) with maximum c_s=0.01, the solid concentration was not negligible in the performed experiment. However, the average value of c_s does not exceed the maximum value of 0.05, proposed by Armanini et al. (2009) for the validity of the quasi-two-phase approach.

https://doi.org/10.5194/egusphere-2024-414
Preprint. Discussion started: 6 September 2024

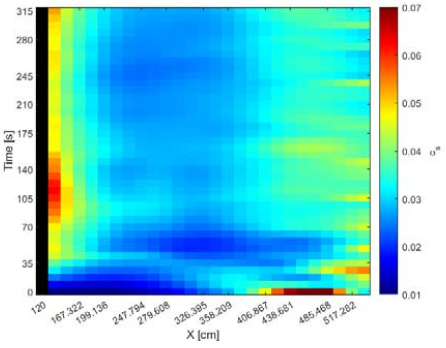

Figure 7. Smoothened color gradient map of the volumetric solid concentration.

5.4 Correlations between the two types of celerities and the Froude number

Figure 8 shows the correlation between the Froude number and the dimensionless local and instantaneous celerity of aggradation during the experiment. For the sake of this comparison, the Fr map of Fig. 4 was also smoothened as those of Fig. 5 and 6. Since the celerity tends to zero after the achievement of an equilibrium condition, only the points for $t < 190$ s are included in this plot. A general decrease of dimensionless celerity for increasing Froude number is observed. An opposite trend is evident for the highest points in the scatter, that are related to the initial stages of the experiment with a flow rate that was still increasing to the test value (this opposite trend is present also in the correlation plots that will be shown later, but will not be discussed again).

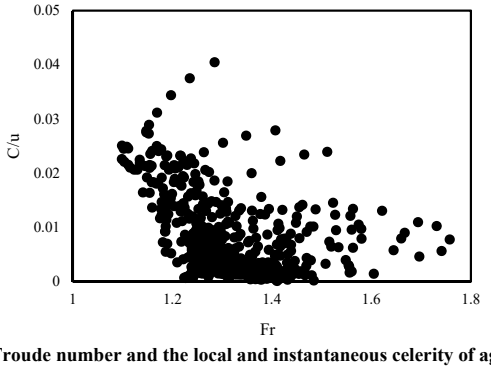

Figure 8. Correlation between the Froude number and the local and instantaneous celerity of aggradation.

The relationships between the Froude number and the dimensionless eigenvalues are presented in Fig. 9 for both the Goutière et al.'s and Morris and Williams' approaches. This depiction corresponds to the typical curves shown in mathematical studies (e.g., Lyn and Altinakar, 2002; Garegnani et al., 2013), the values coming in this case from experimental parameters. The results further demonstrate the difference between the values obtained for λ_2 considering or discarding the sediment concentration.

https://doi.org/10.5194/egusphere-2024-414
Preprint. Discussion started: 6 September 2024

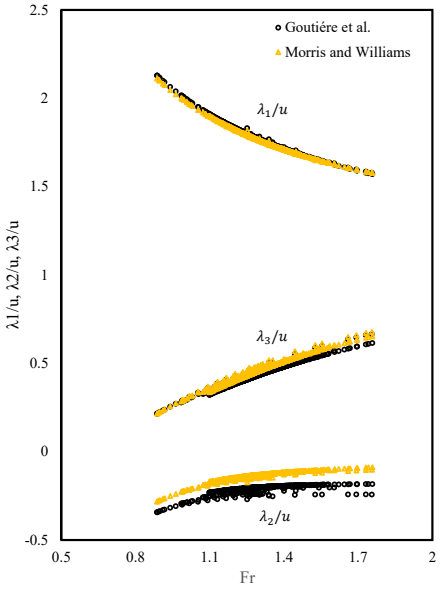

Figure 9. Correlation between the Froude number and the dimensionless eigenvalues.

330

https://doi.org/10.5194/egusphere-2024-414
Preprint. Discussion started: 6 September 2024

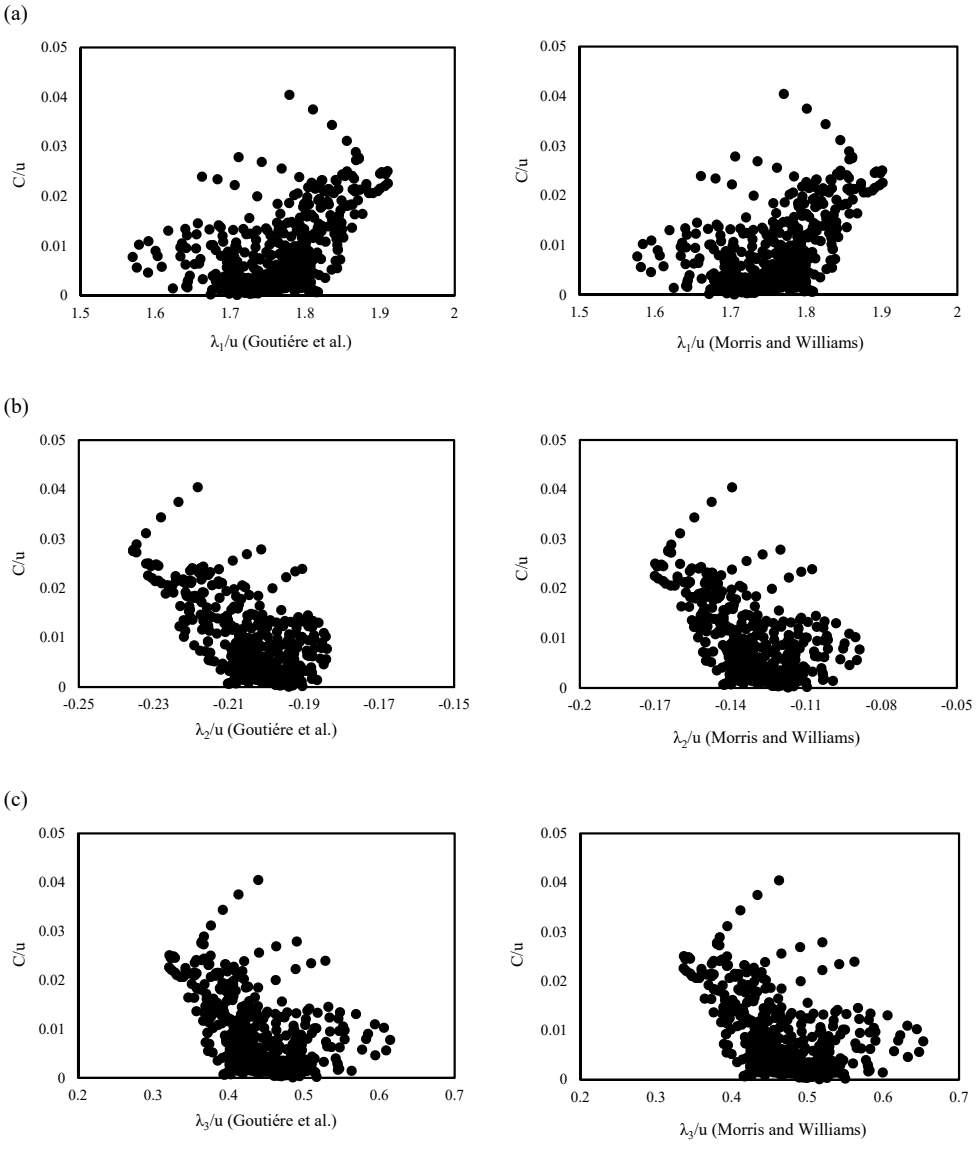

Figure 10. Correlations between the dimensionless eigenvalues and celerity of the aggradation wave. The left graphs are obtained from the approximated solutions proposed by Goutière et al. (2008) and, the right graphs are derived from the exact solution of Morris and Williams' (1996) approach.

Finally, Fig. 10(a, b, and c) shows how the dimensionless celerity of small perturbations and the dimensionless celerity of aggradation correlate with one another, again for both the Goutière et al.'s and Morris and Williams' approaches (left and right panels, respectively). The dimensionless celerity of aggradation increases with dimensionless λ_1 and with the module of dimensionless λ_2 (that is negative), while it decreases with dimensionless λ_3.

6 Discussion

The measurement and analysis methods used in the present manuscript have enabled a depiction of the spatial and temporal evolutions of various quantities. In particular, based on experimental parameters, a local and instantaneous determination was

https://doi.org/10.5194/egusphere-2024-414
Preprint. Discussion started: 6 September 2024

achieved for the celerity of propagation of an aggradation wave and the eigenvalues of the equations modeling the process, representative of the celerity of small perturbations.

We have shown three types of correlation plots: $Fr - \lambda/u$ (Fig. 9), $Fr - C/u$ (Fig. 8), $\lambda/u - C/u$ (Fig. 10). The different trends of correlation are obviously consistent with one another. The first one has been already presented and discussed in works related to the mathematical modelling of the hydro-morphologic process. The others, involving C as determined by Eq. (20), are instead an original depiction of this study.

The second correlation ($Fr - C/u$) has returned the dimensionless celerity as a decreasing function of the Froude number. On the one hand, this reflects the obvious tendencies (i) of the Froude number to increase during an experiment (because the channel needs to achieve a sediment transport capacity equal to the imposed feeding rate by increasing its slope) and (ii) of the celerity towards a zero value at morphological equilibrium. On the other hand, one would expect propagation to be enhanced by an increasing velocity, but this may be somehow masked by any scale used for normalization. Indeed, the appearance of u at the numerator of Fr and at the denominator of C/u has determined the obtained trend because, evidently, with increasing flow velocity, C was increasing less than u.

The trends ($\lambda_i/u - C/u$) depict the relationship between the celerity of small perturbations and that of the aggradation wave. The first eigenvalue, λ_1, is (positive and thus) directed to the downstream; reasonably, one would attribute to it an enhancement of downstream propagation. In fact, this is the detected trend (Fig. 10a). This eigenvalue is normally attributed to water surface perturbations (De Vries, 1965, 1971, 1973, 1993; Sieben, 1997, 1999; Lyn and Altinakar, 2002; Rosatti and Fraccarollo, 2006; Goutière et al., 2008; Armanini, 2018), but a higher velocity will also induce a higher celerity of sediment aggradation. The eigenvalues λ_2 and/or λ_3 are instead attributed to bed perturbations; in this regard, as mentioned above, while De Vries (1965, 1971, 1973, 1993) discussed that just λ_3 is the celerity of bed surface perturbations, Goutière et al. (2008) and Armanini (2018) concluded that λ_2 and λ_3 correspond to bed perturbations, and Lyn and Altinakar (2002) and Sieben (1997,1999) argued that λ_2 and λ_3 may be attributed to both bed and water surface perturbations in near-critical conditions. The eigenvalue λ_2 is directed to the upstream and thus one would think that a higher $|\lambda_2|$ value would induce lower C. The result is contrary to this expectation. Finally, λ_3 is directed to the downstream, but an increase of λ_3 determines a reduction of C, again challenging the interpretation of the result. However, one may consider two aspects: (i) the Froude number increases as time goes on, and (ii) the data points corresponding with higher C/u values are associated with the early stages of the experiment; therefore, the initial time of the experiment in Fig. 10(a) is positioned on the right side of the graphs and in Fig. 10(b) and 10(c) is located on the left side of the graphs. As mentioned, the dimensionless celerity has a decreasing relationship with the Froude number (Fig. 8) and decreases during the experiment. Considering the two above-mentioned aspects, this trend can be recognized also in all graphs of Fig. 10. Furthermore, Fig. 9 shows that, while λ_1 and $|\lambda_2|$ decrease with Fr, λ_3 increases with Fr. Once again, by considering the mentioned aspects, these relationships between λ_i and Fr are realized in the graphs of Fig. 10, where, λ_1 and $|\lambda_2|$ decrease as time elapses (which coincides with increasing Fr) and, λ_3 increases over time. In summary, one may conclude that the celerities of small perturbations are linked to the celerity of the aggradation wave through the Froude number.

In the context of a relationship between the λ and C, the possibility or not to discard the sediment concentration while expressing the eigenvalues loses its merit. Obviously, formulating the eigenvalues with or without concentration changes their values (even by 50 – 100% for λ_2, that is the eigenvalue most affected by the sediment concentration), but it will be always possible to find a trend linking the celerities of small perturbations and the celerity of the aggradation wave.

The points before the water discharge achieves its nominal value show opposite trends to the others. The approaches introduced above are for unsteady flows, so the different trend cannot be attributed to a limitation of the mathematical depiction. The different trend thus needs to be attributed to the swift change of the flow rate at the very beginning of the experiment.

The celerities of the two types are largely different in value (as an example for all, this is conceptually expected for the properties of the quantities at equilibrium, where C tends to 0 while the eigenvalues do not) and follow a general trend like the smaller, the faster, spotted in different ways also for other processes (e.g., Lanzoni et al., 2006; Radice, 2021). From an

https://doi.org/10.5194/egusphere-2024-414
Preprint. Discussion started: 6 September 2024

engineering point of view, the mismatch means that one cannot rely on the eigenvalues to determine when sediment supplied into a river will create problems at any certain point (because the estimate would result in negligible time available for action), and gives merit to the experimental determination of the celerity of propagation of the aggradation wave. A bulk result obtained in the present work is that C/u is less than 0.04. This result, shown here for a single experiment, was confirmed by the others run in the current experimental campaign. This is a crucial piece of information one needs to assess if supplied sediment will reach some key spots along a channel. Extensive analysis will reveal how this bulk celerity may depend on the control parameters, following earlier investigations for sediment plumes or fronts under subcritical flow.

Finally, the system of the governing differential equations has been considered in this study in terms of its eigenvalues. The literature shows that several research efforts have been focused on simplifying the above-mentioned hyperbolic system of partial differential equations to a single parabolic diffusion equation and presenting an analytical solution for this simplified equation, under the main assumptions of quasi-steady flow, quasi-uniform flow conditions, and the constancy of the roughness coefficient (e.g., Culling, 1960; Soni et al., 1980; Gill, 1983; Jaramillo and Jain, 1984; Zhang and Kahawita, 1987). The existence of these contributions offers additional means for comparison and interpretation of the present experimental results.

7 Conclusions

If a high detail is maintained in an aggradation experiment for measuring the bed and water surface elevations in space and time, a corresponding spatial and temporal evolution can be obtained for a celerity of propagation of the aggradation wave. Besides, an analogous quantification can be obtained for the eigenvalues of the governing equations under a quasi-two-phase approach, these eigenvalues representing the celerity of small perturbations.

The analysis performed in the present work has been focused on the correlation between the celerities of the two types and has led to the following major conclusions:

(i) The celerity of aggradation is correlated with the eigenvalues through the Froude number and the general trends show C increasing with λ_1 and $|\lambda_2|$ and decreasing with λ_3.

(ii) Even though there is a correlation between the C and λ, they are largely different in magnitude, with the celerity of the aggradation wave being much smaller than the others.

(iii) From a mathematical point of view, using a model that considers or not the solid concentration may obviously lead to different results for the eigenvalues of the system (while λ_1 is almost the same for the two approaches and a slight difference exists in λ_3, a major difference is observed for λ_2 that has a higher absolute value when the concentration is discarded). However, considering or not solid concentration in the governing equations does not affect the qualitative relationships between the different celerities.

(iv) The celerity of aggradation, C, is in the order of 10^{-2} times the bulk water velocity for the aggradation process simulated in the laboratory run that was used in this study.

Data availability statement

The raw data of the experiment are provided here: https://doi.org/10.5281/zenodo.10641001.

Author contribution

Conceptualization: H.E., A.R.; Methodology: H.E., A.R.; Software: E.P., E.Z.; Formal analysis and Visualization: H.E., E.P., M.H., K.T., M.Y.N., E.Z., R.Z.; Writing – original draft preparation: H.E.; Writing: review & editing: H.E., A.R.; Funding acquisition: A.R.

https://doi.org/10.5194/egusphere-2024-414
Preprint. Discussion started: 6 September 2024

Competing interests

The authors declare that they have no conflict of interest.

Acknowledgments

The present study has been financially supported by the Italian Ministry of University and Research through the Ph.D. scholarship of H.E. and by the European Union – Next Generation EU through the PRIN project "Sediment Transport REsearch for cAtchments Management" (STREAM), project no. 2022SAFKS4.

References

Aksoy, H., & Kavvas, M. L. (2005). A review of hillslope and watershed scale erosion and sediment transport models. *CATENA*, *64*(2), 247–271. https://doi.org/10.1016/j.catena.2005.08.008

Alves, E., & Cardoso, A. (1999). Experimental study on aggradation. *Int. J. Sediment Res.*, *14*(1): 1-15

Ancey, C. (2020). Bedload transport: a walk between randomness and determinism. Part 1. The state of the art. *Journal of Hydraulic Research*, *58*(1), 1–17. https://doi.org/10.1080/00221686.2019.1702594

Armanini, A. (2018). Principles of River Hydraulics. Chapter 7. Mathematical Models of Riverbed Evolution (pp. 131–172). *Springer International Publishing*. https://doi.org/10.1007/978-3-319-68101-6_7

Armanini, A., Fraccarollo, L., & Rosatti, G. (2009). Two-dimensional simulation of debris flows in erodible channels. *Computers & Geosciences*, *35*(5), 993–1006. https://doi.org/10.1016/j.cageo.2007.11.008

Armanini, A., &Di Silvio, G. (1988). A one-dimensional model for the transport of a sediment mixture in non-equilibrium conditions. *Journal of Hydraulic Research*, *26*(3), 275–292. https://doi.org/10.1080/00221688809499212

Chow, V. T., Maidment, D. R. & Mays, L. W. (1988). *Applied hydrology*. McGraw-Hill. ISBN: 0070108102.

Cui, Y., & Parker, G. (2005). Numerical Model of Sediment Pulses and Sediment-Supply Disturbances in Mountain Rivers. *Journal of Hydraulic Engineering*, *131*(8), 646–656. https://doi.org/10.1061/(ASCE)0733-9429(2005)131:8(646)

Cui, Y., Parker, G., Lisle, T. E., Gott, J., Hansler-Ball, M. E., Pizzuto, J. E., Allmendinger, N. E., & Reed, J. M. (2003). Sediment pulses in mountain rivers: 1. Experiments. *Water Resources Research*, *39*(9). https://doi.org/10.1029/2002WR001803

Culling, W. E. H. (1960). Analytical theory of erosion. *Journal of Geology*, *68*(3), 336-344. https://doi.org/10.1086/626663

de Vries, M. (1965). Consideration about non-steady bed-load-transport in open channels. *Proc. of the 11th Congress of IAHR*, Leningrad, 3.8.1–3.8.8

de Vries, M. (1971). Solving river problems by hydraulic and mathematical models. *Delft Hydraulic Laboratory Publications*, Delft, The Netherlands

de Vries, M. (1973). River-bed variations-aggradation and degradation. *Delft Hydraulic Laboratory Publications*, Delft, The Netherlands

de Vries, M. (1993). River Engineering: Lecture notes f10. *Delft University of Technology, Faculty of Civil Engineering Department of Hydraulic Engineering,* Delft, The Netherlands

Dotterweich, M. (2008). The history of soil erosion and fluvial deposits in small catchments of central Europe: Deciphering the long-term interaction between humans and the environment — A review. *Geomorphology*, *101*(1), 192–208. https://doi.org/10.1016/j.geomorph.2008.05.023

Eslami, H., Yousefyani, H., Yavary Nia, M., & Radice, A. (2022). On how defining and measuring a channel bed elevation impacts key quantities in sediment overloading with supercritical flow. *Acta Geophysica*, *70*(5), 2511–2528. https://doi.org/10.1007/s11600-022-00851-2

https://doi.org/10.5194/egusphere-2024-414
Preprint. Discussion started: 6 September 2024

Garegnani, G., Rosatti, G., & Bonaventura, L. (2011). Free surface flows over mobile bed: Mathematical analysis and numerical modeling of coupled and decoupled approaches. *Communications in Applied and Industrial Mathematics*, *2*(1), 1-22. https://doi.org/10.1685/journal.caim.371

Garegnani, G., Rosatti, G., & Bonaventura, L. (2013). On the range of validity of the Exner-based models for mobile-bed river flow simulations. *Journal of Hydraulic Research*, *51*(4), 380–391. https://doi.org/10.1080/00221686.2013.791647

Gill, M. A. (1983). Diffusion model for aggrading channels. *Journal of Hydraulic Research*, *21*(5), 355-367. https://doi:10.1080/00221688309499457

Goutière, L., Soares-Frazão, S., Savary, C., Laraichi, T., & Zech, Y. (2008). One-Dimensional Model for Transient Flows Involving Bed-Load Sediment Transport and Changes in Flow Regimes. *Journal of Hydraulic Engineering*, *134*(6), 726–735. https://doi.org/10.1061/(ASCE)0733-9429(2008)134:6(726)

Greco, M., Iervolino, M., Leopardi, A., & Vacca, A. (2012). A two-phase model for fast geomorphic shallow flows. *International Journal of Sediment Research*, *27*(4), 409–425. https://doi.org/10.1016/S1001-6279(13)60001-3

Haddadchi, A., Nosrati, K., & Ahmadi, F. (2014). Differences between the source contribution of bed material and suspended sediments in a mountainous agricultural catchment of western Iran. *CATENA*, *116*, 105–113. https://doi.org/10.1016/j.catena.2013.12.011

Jain, S.C. (2001). *Open-channel flow*. John Wiley & Sons, ISBN: 0471356417.

Jaramillo, W. F., & Jain, S.C. (1984). Aggradation and degradation of alluvial-channel beds. *Journal of Hydraulic Engineering*, *110*(8), 1072–1085. https://doi:10.1061/(ASCE)0733-9429(1984)110:8(1072)

Kassem, A. A., & Chaudhry, M. H. (1998). Comparison of coupled and semicoupled numerical models for alluvial channels. *Journal of Hydraulic Engineering*, *124*(8), 794–802. https://doi.org/10.1061/(ASCE)0733-9429(1998)124:8(794)

Lane, S. N., Tayefi, V., Reid, S. C., Yu, D., & Hardy, R. J. (2007). Interactions between sediment delivery, channel change, climate change and flood risk in a temperate upland environment. *Earth Surface Processes and Landforms*, *32*(3), 429–446. https://doi.org/10.1002/esp.1404

Lanzoni, S., Siviglia, A., Frascati, A., & Seminara, G. (2006). Long waves in erodible channels and morphodynamic influence. *Water Resources Research , 42*(6). https://doi:10.1029/2006WR004916

Lee, H.-Y., & Hsieh, H. (2003). Numerical simulations of scour and deposition in a channel network. *International Journal of Sediment Research*, *18*(1), 32-49.

Lisle, T. E., Cui, Y., Parker, G., Pizzuto, J. E., & Dodd, A. M. (2001). The dominance of dispersion in the evolution of bed material waves in gravel-bed rivers. *Earth Surface Processes and Landforms*, *26*(13), 1409–1420. https://doi.org/10.1002/esp.300

Longoni, L., Papini, M., Brambilla, D., Barazzetti, L., Roncoroni, F., Scaioni, M., & Ivanov, V. I. (2016). Monitoring riverbank erosion in mountain catchments using terrestrial laser scanning. *Remote Sensing*, *8*(3), 241. https://doi.org/10.3390/rs8030241

Lyn, D. A. (1987). Unsteady sediment-transport modeling. *Journal of Hydraulic Engineering*, *113*(1), 1–15. https://doi.org/10.1061/(ASCE)0733-9429(1987)113:1(1)

Lyn, D. A., & Altinakar, M. (2002). St. Venant–Exner equations for near-critical and transcritical flows. *Journal of Hydraulic Engineering*, *128*(6), 579–587. https://doi.org/10.1061/(ASCE)0733-9429(2002)128:6(579)

Mazzorana, B., Comiti, F., & Fuchs, S. (2013). A structured approach to enhance flood hazard assessment in mountain streams. *Natural Hazards*, *67*(3), 991–1009. https://doi.org/10.1007/s11069-011-9811-y

Morris, P. H., & Williams, D. J. (1996). Relative celerities of mobile bed flows with finite solids concentrations. *Journal of Hydraulic Engineering*, *122*(6), 311–315. https://doi.org/10.1061/(ASCE)0733-9429(1996)122:6(311)

Pizarro, A., Manfreda, S., & Tubaldi, E. (2020). The science behind scour at bridge foundations: A review. *Water*, *12*(2). https://doi.org/10.3390/w12020374

https://doi.org/10.5194/egusphere-2024-414
Preprint. Discussion started: 6 September 2024

Radice, A. (2021). An experimental investigation of sediment kinematics and multi-scale propagation for laboratory bed-load dunes. Sedimentology, *68*(7), 3476–3493. https://doi.org/10.1111/sed.12906

Radice, A., & Zanchi, B. (2018). Multicamera, multimethod measurements for hydromorphologic laboratory experiments. *Geosciences*, *8*. https://doi.org/ 10.3390/geosciences8050172

Radice, A., Rosatti, G., Ballio, F., Franzetti, S., Mauri, M., Spagnolatti, M., & Garegnani, G. (2013). Management of flood hazard via hydro-morphological river modelling. The case of the Mallero in Italian Alps. *Journal of Flood Risk Management*, *6*(3), 197–209. https://doi.org/10.1111/j.1753-318X.2012.01170.x

Rosatti, G., Chemotti, R., & Bonaventura, L. (2005). High order interpolation methods for semi-Lagrangian models of mobile-bed hydrodynamics on Cartesian grids with cut cells. *International Journal for Numerical Methods in Fluids*, *47*(10-11), 1269–1275. https://doi.org/10.1002/fld.910

Rosatti, G., & Fraccarollo, L. (2006). A well-balanced approach for flows over mobile-bed with high sediment-transport. *Journal of Computational Physics*, *220*(1), 312–338. https://doi.org/10.1016/j.jcp.2006.05.012

Sear, D. A., Newson, M. D., & Brookes, A. (1995). Sediment-related river maintenance: The role of fluvial geomorphology. *Earth Surface Processes and Landforms*, *20*(7), 629–647. https://doi.org/10.1002/esp.3290200706

Sieben, J. (1997). Modelling of Hydraulics and Morphology in Mountain Rivers. PHD thesis, *Delft University of Technology, Faculty of Civil Engineering*, Delft, The Netherlands

Sieben, J. (1999). A theoretical analysis of discontinuous flow with mobile bed. *Journal of Hydraulic Research*, *37*(2), 199–212. https://doi.org/10.1080/00221689909498306

Sklar, L. S., Fadde, J., Venditti, J. G., Nelson, P., Wydzga, M. A., Cui, Y., & Dietrich, W. E. (2009). Translation and dispersion of sediment pulses in flume experiments simulating gravel augmentation below dams. *Water Resources Research*, *45*(8). https://doi.org/10.1029/2008WR007346

Soni, J. P., Garde, R. J., & Ranga Raju, K. G. (1980). Aggradation in streams due to overloading. *Journal of the Hydraulics Division, ASCE, 106*(1), 117-132. https://doi: 10.1061/JYCEAJ.0005338

Soni, J. P. (1981). Laboratory study of aggradation in alluvial channels. *Journal of Hydrology*, *49*(1), 87–106. https://doi.org/10.1016/0022-1694(81)90207-9

Stover, S. C., & Montgomery, D. R. (2001). Channel change and flooding, Skokomish River, Washington. *Journal of Hydrology*, *243*(3), 272–286. https://doi.org/10.1016/S0022-1694(00)00421-2

Unigarro Villota, S. (2017). Laboratory study of channel aggradation due to overloading

Yen, C., Chang, S., & Lee, H. (1992). Aggradation-degradation process in alluvial channels. *Journal of Hydraulic Engineering*, *118*(12), 1651–1669. https://doi.org/10.1061/(ASCE)0733-9429(1992)118:12(1651)

Zanchi, B., & Radice, A. (2021). Celerity and height of aggradation fronts in gravel-bed laboratory channel. *Journal of Hydraulic Engineering*, *147*(10), 4021034. https://doi.org/10.1061/(ASCE)HY.1943-7900.0001923

Zhang, H., & Kahawita, R. (1987). Nonlinear model for aggradation in alluvial channels. *Journal of Hydraulic Engineering*, *113*(3), 353–369. https://doi.org/ 10.1061/(ASCE)0733-9429(1987)113:3(353)